On the Dynamics and Conformation of the HA2 Domain of the Influenza Virus Hemagglutinin†

Chul-Hyun Kim, Jed C. Macosko, Yeon Gyu Yu, and Yeon-Kyun Shin*

Department of Chemistry, University of California, Berkeley, California 94720

Received February 12, 1996; Revised Manuscript Received March 14, 1996⊗

ABSTRACT: To investigate the dynamics and conformation of the membrane-interacting HA2 domain of the hemagglutinin protein of influenza virus, the peripheral part of the HA2 domain (aa 1−127) was expressed in *Escherichia coli*. Four consecutive single-cysteine mutants, F63C, H64C, Q65C, and I66C, were generated using site-directed mutagenesis. This region is proposed to undergo a conformational change from a loop to a helical coiled-coil when going from the native to the fusion-active state [Bullough *et al*. (1994) *Nature (London) 371*, 37−43]. In the trimeric coiled-coil geometry positions 63 and 66 belong to the core so that cysteines from individual monomers are spatially close. On the other hand, positions 64 and 65 face the aqueous phase so that cyteines from monomers are spatially remote. The mutants were studied with cysteine−cysteine cross-linking and the spin-labeling electron paramagnetic resonance (EPR) in both the membrane-bound state and in the detergent-solubilized state. Extensive intramolecular cysteine−cysteine cross-linking was observed not only for F63C and I66C but also for H64C. Rates of cross-linking were comparable for these three mutants at physiological temperatures. These results are inconsistent with what is expected for a well-defined coiled-coil and suggest that the region containing the mutation sites is flexible. However, a characteristic cross-linking pattern consistent with a well-defined coiled-coil developed at very low temperatures. Line shapes of EPR spectra also indicate that this region is dynamic at ambient temperatures. Such flexibility perhaps arises from an equilibrium between a coiled-coil and a random coil conformation. No significant changes of the EPR spectra were observed upon lowering the pH to fusogenic conditions, suggesting that this flexible structure is the stable conformation at both neutral and low pH. The dynamic flexibility of this region may have important implications for the mechanism of HA-induced membrane fusion; for example it may be required for the apposition of the viral and endosomal membranes.

The influenza virus surface is coated with a hemagglutinin (HA) protein. Virus infection begins with the binding of HA to sialic acid receptors on the surface of the target cell. After the internalization of the virus through receptor-mediated endocytosis (Maltin *et al.*, 1981), HA mediates the fusion of the viral membrane with the endosomal membrane to allow the passage of the viral genome into the host cytoplasm. A key step in this fusion process is the activation of HA from the native state to the fusogenic state (Skehel *et al.*, 1982). This transition is triggered by the mildly acidic pH in the mature endosome [for review, see Wiley and Skehel (1987), White (1992), and Stegmann and Helenius (1993)].

In the native state, HA is a homotrimer consisting of two subunits, the receptor-binding HA1 domain and the membrane-interacting HA2 domain (Wilson *et al.*, 1981). The HA2 domain contains a NH_2-terminal hydrophobic sequence, called the "fusion peptide", that interacts with the target membrane during membrane fusion (Stegmann *et al.*, 1991; Tsurudome *et al.*, 1992). Part of the HA2 domain forms a hairpin-loop. This loop connects a short α-helix near the fusion peptide to a long helical stem in the COOH-terminal region which protrudes from the viral membrane. Three such long helices assemble into a three-stranded coiled-coil that forms the core of the HA homotrimer. The most intriguing feature of the structure of native HA is that the fusion peptide is tucked inside of the protein, nearly 100 Å away from the top of the molecule (Wilson *et al.*, 1981).

There is evidence that under mildly acidic conditions, the hydrophobic fusion peptide region is exposed to the aqueous phase so that it can interact with the target membrane (Skehel *et al.*, 1982; Doms & Helenius, 1986; White & Wilson, 1987; Stegmann *et al.*, 1990). However, it is not clear what the global conformation of HA is in this fusogenic state. One model proposes a localized conformational change: exposure of the fusion peptide while maintaining the intact hairpin structure (Stegmann *et al.*, 1990). Upon the conformational change, the fusion peptide moves out of the protein interior but is still nearly 100 Å away from the target membrane. Then the question arises as to how this fusion peptide interacts with the distal membrane. It is proposed that the HA trimer tilts to present its fusion peptide to the target membrane (Stegmann *et al.*, 1990). Interestingly, no global structural change was observed for the Japan strain influenza virus after low-pH pretreatment when examined by electron microscopy (Puri *et al.*, 1990).

Recently, another model that assumes a global conformational change has emerged. This model is based on structural predictions (Carr & Kim, 1993) and crystallographic studies (Bullough *et al.*, 1994). This model proposes that the loop region in the hairpin structure undergoes a conformational

† This work was supported by NIH Grant GM51290-02, ACS PRF 28160-G7, and UC Berkeley Chancellor's Initiative Grant. Y.-K.S. is a 1995 Searle Scholar.

* To whom correspondence should be addressed.

⊗ Abstract published in *Advance ACS Abstracts,* April 15, 1996.

S0006-2960(96)00332-7 CCC: $12.00

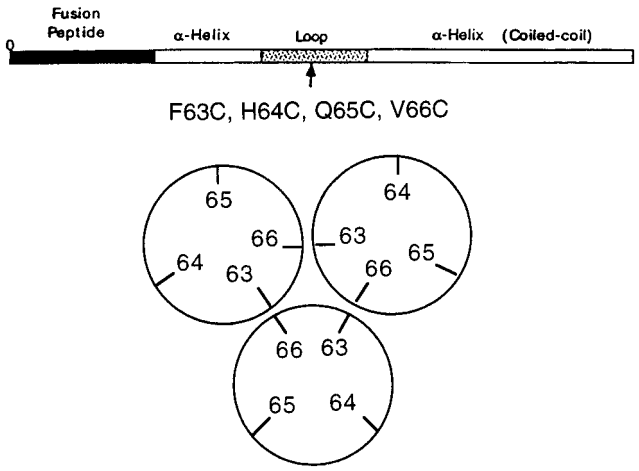

FIGURE 1: (Top) Schematic diagram of the structural units in the native structure of HA2. (Bottom) Trimeric helical wheel diagram taken from the low-pH crystal structure (Bullough *et al.*, 1994) shows the arrangement of the positions, **a**−**d**, of the four cysteine mutants used in this study.

change to a helix, thereby extending the trimeric stem straight up and allowing the fusion peptide to relocate toward the top of the ectodomain. In fact, an elongation of the molecular length of HA of the X-31 strain influenza virus was observed upon pretreatment with acidic pH (Ruigrok *et al.*, 1986). However, the crystallographic study was based on a fragment which was proteolytically cleaved from the viral membrane and was further cleaved to delete the fusion peptide region to prevent aggregation (Bullough *et al.*, 1994).

Crucial to the understanding of HA-induced membrane fusion is the role of the fusion peptide (Daniels *et al.*, 1985; Gething *et al.*, 1986). In this work, the conformation and the dynamics of a portion of the HA2 domain containing the fusion peptide (aa 1−127: FHA2, see Figure 1) was investigated both in detergent and in the membrane using site-specific cysteine−cysteine (cys−cys) cross-linking experiments and spin-labeling electron paramagnetic resonance (EPR)[1] spectroscopy. These two techniques have proven useful in studying secondary, tertiary, and quaternary structures of proteins (Falke & Koshland, 1987; Milligan & Koshland, 1988; Yu *et al.*, 1995; Hubbell & Altenbach, 1994; Millhauser, 1992; Rabenstein & Shin, 1995b). For FHA2 the cysteine scanning experiments as well as the nitroxide scanning experiments indicated that the region proposed to undergo a loop-to-helix conformational change is dynamic and flexible under physiological conditions. In addition, no significant conformational change has been observed with EPR in this region upon acidification, indicating that such flexible conformation is the thermodynamically stable structure under both neutral and acidic pH. Thus, it is likely that the loop region of the HA2 domain in the fusogenic state remains flexible, neither being a hairpin nor a well-defined coiled-coil. The flexibility and the dynamic structure of this region may have important implications for the mechanism of HA-induced membrane fusion. For instance, flexibility may be required for the apposition of the viral and cell membranes.

MATERIALS AND METHODS

Materials. FHA2 and its site-specific cysteine mutant proteins were all expressed in *Escherichia coli*. The strain used for expression of plasmids bearing FHA2 was *E. coli* BL21(DE3) pAcyc [*hsdS gal* (λcIts857 *ind* 1 Sam7 *nin* 5 *lac* UV5-T7 gene*1*)]. The original gene for the soluble part of the HA2 domain (aa 33−127) was kindly provided by Dr. Peter S. Kim at MIT. The NH_2-terminal region (aa 1−32) was inserted onto the original gene, and for overexpression and site-specific mutagenesis we subcloned it into the pET 21a(+) plasmid vector which was purchased from Novagen (Madison, WI). For the plasmid purification and amplification, we used the *E. coli* strain DH5α [*sup*E44 Δ*lac* U169 (*ϕ*80 *lac* ZΔM15) *hsd* R17 *rec* A1 *end* A1 *gyr* A96 *thi* −1 *rel* A1]. For single-strand DNA preparation, we used the *E. coli* strain CJ236 [*dut* 1 *ung* 1 *thi* −1 *rel* A1/ pCJ105(cam^r F′)]. Isopropyl β-D-thiogalactopyranoside (IPTG) was purchased from United States Biochemical (Cleveland, OH). *n*-Octyl β-D-glucoside (OG) was purchased from Anatrace (Maumee, OH) and 1,10-phenanthroline (phe) monohydrate was purchased from Sigma (St. Louis, MO). 1-Palmitoyl-2-oleoylphosphatidylcholine (POPC) and 1-palmitoyl-2-oleoylphosphatidylglycerol (POPG) were purchased from Avanti Polar Lipids (Birmingham, AL). *S*-(1-Oxy-2,2,5,5-tetramethylpyrroline-3-methyl)methanethiosulfonate (MTSSL) spin label was from Reanal (Hungary), and α-^{35}S-dATP was from Amersham (Arlington Height, IL). Q-Sepharose fast flow resin and DEAE Sepharose fast flow resin were purchased from Pharmacia Biotech (Uppsala, Sweden).

Expression. Purified plasmids were transferred into *E. coli* BL21(DE3) pAcyc using the $CaCl_2$ bacterial transformation method. The cells were grown on LB/A/K plates (Luria broth agar, 100 μg of ampicillin/mL, 25 μg of kanamycin/mL) overnight. A single colony was selected and grown in 50 mL of LB/A/K broth media at 37 °C until they reached the exponential phase. The culture was centrifuged at 5000*g* for 10 min, resuspended in fresh LB/A/K broth media, and transferred to 1.5 L of LB/A/K broth media. After 3−4 h of growth at 37 °C, the density of the cell culture was estimated by measuring the optical density at 600 nm (OD_{600}). At $OD_{600} = 1.0$, the culture was induced with 0.5 mM (final concentration) IPTG. After 2−3 h, the culture was harvested by centrifugation (5000*g*) at 4 °C and analyzed on a protein gel. The expression level of FHA2 was approximately 20% of the cell protein. For purification, the cell pellet was stored at −80 °C in 5 mM citrate−phosphate buffer (pH = 7.0) which contains 1mM EDTA, 1 mM PMSF, 4 mM DTT, and 150 mM NaCl (buffer A).

Purification. The cell pellet was resuspended in buffer A with 25 μM DNase I. The resuspended cell pellet was immediately French pressed at 12 000 psi 2−3 times. The crude cell extract was centrifuged at 4 °C at 5000*g* for 10 min and then at 10 000*g* for 15 min two times. Each time a portion of the resulting pellet was saved for SDS polyacrylamide gel electrophoresis (PAGE) and the supernatant was transferred for the next step. After the second 15 min centrifugation, the supernatant was transferred to an ultracentrifuge tube and spun 1 h at 100 000*g* and 4 °C. This resulting pellet was the *E. coli* plasma membrane fraction.

[1] Abbreviations: CD, circular dichroism; Cys, cysteine; Phe, 1,10-phenanthroline; PAGE, polyacrylamide gel electrophoresis; EPR, electron paramagnetic resonance; MTSSL, *S*-(1-oxy-2,2,5,5-tetramethylpyrroline-3-methyl)methanethiosulfonate spin label; PMSF, phenylmethanesulfonyl fluoride; IPTG, isopropyl β-thiogalactopyranoside; OG, *n*-octyl β-D-glucoside; POPC, 1-palmitoyl-2-oleoylphosphatidylcholine; POPG, 1-palmitoyl-2-oleoylphosphatidylglycerol; LB, Luria broth media; OD_{600}, optical density at 600nm.

All the fractions were analyzed on a 15% SDS−PAGE gel, and it was found that FHA2 was in the membrane fraction and constituted about 50% of the membrane protein. This membrane fraction was resuspended in Buffer A using a glass homogenizer and then solubilized with 1% OG and centrifuged at 100 000*g* for 1 h. The supernatant was loaded on a DEAE Sepharose gravity column equilibrated in buffer A which contained 2% OG. Using a NaCl gradient from 150 to 600 mM, FHA2 was purified up to 90% and with a second Q-Sepharose gravity column using the same NaCl gradient, the purity achieved was more than 95%. The net yield was approximately 3−4 mg/1.5 L of culture.

Site-Directed Mutagenesis. In the full-length HA2 domain there are several native cysteines. However, all these cysteines are in the COOH-terminal region and not in residues 1−127. Cysteine mutants of FHA2 were generated using the method described by Kunkel (1985). Figure 1 shows each mutation site in the FHA2 construct. The sequences of the DNA for the wild type and all four mutants (F63C, H64C, Q65C, and I66C) were confirmed by DNA sequencing using the sequenase version 2.0 DNA sequencing kit (United States Biochemical, Cleveland, OH).

Site Specific Cys−Cys Cross-Linking. Samples used in the cys−cys cross-linking experiments were stored at −80 °C in buffer A with 2% OG. Just prior to cross-linking, the sample was thawed. DTT removal and buffer exchange were achieved with a Bio-Rad DG10 desalting column (Bio-Rad, Hercules, CA). For the cross-linking reaction, 50 mM Tris buffer (pH = 7.2) was used. After the buffer exchange, Cu(II)(1,10-phenanthroline)$_3$ (Cu(II)(phe)$_3$) was added to protein samples to initiate the cross-linking reaction. For all experiments the final concentration of Cu(II)(phe)$_3$ was 0.5 mM. Samples were then reacted at 37 °C for different periods of time (25 s to 10 min) and then quenched by the addition of (final concentrations) 12.5 mM *N*-ethylmaleimide and 12.5 mM EDTA in the Laemmli buffer [60 mM Tris buffer (pH 6.8) containing 2% (w/v) SDS, 6% (w/v) sucrose, and 0.005% (w/v) bromophenol blue]. 15% SDS−PAGE gels were used for protein analysis. Cross-linking rates were determined by scanning the gels with a LKB Zenith densitometer (Biomed Instruments Inc., Fullerton, CA).

Chemical Cross-Linking. Nonspecific intrasubunit cross-linking was achieved using glutaraldehyde as a linker. Samples were thawed from −80 °C and were buffer-exchanged into a 20 mM phosphate (pH 8.0) buffer using the Bio-Rad DG10 desalting column. Glutaraldehyde was added to the desired final concentration (0.06−60 mM), and samples were incubated at room temperature for 15 min. The samples were quenched by adding a glycine solution (final concentration = 100 mM) and run on a 15% SDS−PAGE gel.

Circular Dichroism. For CD measurements, the sample buffer was exchanged into buffer A containing 2% OG at pH 7.0. Protein concentration was determined by absorbance at 280 nm and calibrated with FHA2 wild type in 6 M GuHCl (ϵ = 15 220 M^{-1} cm^{-1}). The helicity of the protein samples was measured in a 0.1 cm pathlength quartz cuvette by using the Circular Dichroism Spectrometer model 62 DS (AVIV, Lakewood, NJ).

Site-Specific Spin-Labeling EPR. After removing DTT from the sample, a 4-fold molar excess of MTSSL was added to the solution at pH 8.0. The labeling reaction was completed within 3−4 h at room temperature. The unreacted spin label was then removed with a Bio-Rad DG10 desalting column. EPR measurements were performed at room temperature using a Bruker ESP 300 EPR spectrometer (Bruker, Germany) equipped with a low-noise microwave amplifier (Miteq, Hauppauge, NY) and a loop-gap resonator (Medical Advances, Milwaukee, WI). The modulation amplitude was set at no greater than one-fifth of the line width. Spin concentrations were determined by comparing double integrals of the derivative EPR spectra with that of standard sample made of 100 μM 4-hydroxy-Tempo. For all mutants the labeling ratios were nearly quantitative.

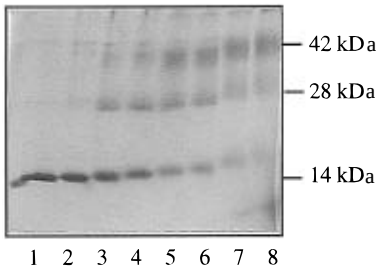

FIGURE 2: SDS−PAGE of the chemical cross-linking experiment shows monomer, dimer, and trimer bands for FHA2. The lack of higher molecular bands and the predominance of the trimer at a saturating concentration (60 mM) of glutaraldehyde indicate FHA2 is a trimer in 2% OG. Concentrations of glutaraldehyde are 0, 0.06, 0.2, 0.6, 2, 6, 20, and 60 mM in lanes 1−8, respectively.

Vesicle Preparation and Reconstitution. Uniformly-sized lipid vesicles (100 nm in diameter) containing 80 mole% POPC and 20 mole% POPG, were made as previously described (Rabenstein & Shin, 1995a). For the reconstitution, the vesicle solution was mixed with OG solubilized protein. The final concentration of lipid in the mixture was 10 mM, and the protein concentration was 10 μM in buffer A containing 1% OG. OG was removed with Bio-Bead SM2 resin (Bio-Rad, Hercules, CA). The resin was added to the mixture at a concentration of 400 mg/mL, and the solution was agitated for 1 h. This procedure was repeated three times. The unreconstituted protein aggregate was then removed by low-speed centrifugation (5000*g*). Finally, the reconstituted vesicles were obtained as a pellet by ultracentrifugation (100 000*g* for 1 h). The pellet was resuspended in buffer A.

RESULTS

Chemical Cross-Linking. HA is a trimeric protein. According to the crystal structure (Wilson *et al.*, 1981), the trimeric long α-helical stem region of the HA2 domain most likely provides the basis for the trimeric organization of the HA protein. Since FHA2 contains this stem region, we might expect that this fragment preserves a trimeric conformation. To find whether this is true, we performed chemical cross-linking experiments using glutaraldehyde chemistry (Habeeb & Hiramoto, 1968). The SDS−PAGE gel in Figure 2 shows the results of the chemical cross-linking of the OG solubilized wild type FHA2. From left to right is shown the effect of increasing glutaraldehyde concentration. As the concentration of glutaraldehyde increased, a band consistent with a trimer developed. This became the major band at high glutaraldehyde concentrations without the appearance of a higher molecular weight band. This strongly indicates that the fragment exists predominantly as a trimer. The chemical cross-linking results were verified for all cysteine mutants (F63C, H64C, Q65C, and I66C), and the results were virtually identical to that of the wild type FHA2.

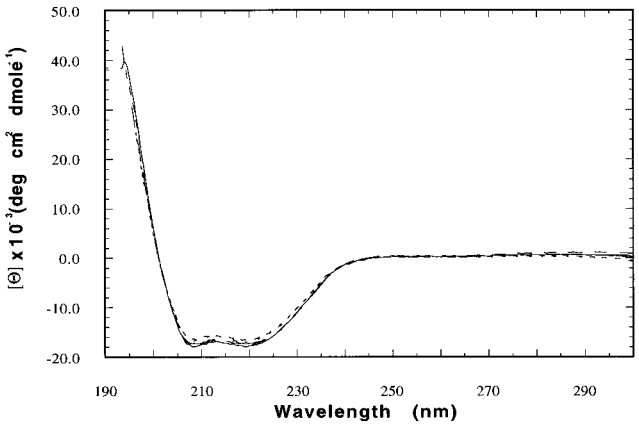

FIGURE 3: Circular dichroism spectra reflect the α-helical nature of wild type FHA2 and four FHA2 cysteine mutants. The average helicity is 49% with a standard deviation of 1.4%. Spectra were recorded at room temperature in 2% OG. A solid line represents wild type FHA2, and broken lines denote the cysteine mutants.

Circular Dichroism. CD experiments were performed to investigate the structural perturbation due to the cysteine mutations. CD spectra of all four cysteine mutants were compared with the spectrum of the wild type (Figure 3). The spectra of all the FHA2 mutants and wild type showed characteristic α-helical features. Also, the CD spectra of all the mutants overlap with the spectrum of the wild type FHA2 within experimental uncertainty, strongly indicating that for all mutants there is essentially no structural perturbation due to the cysteine mutations. The mean ellipticity at 222 nm was −16 700 in units of deg cm^2 dmol^{-1}. Assuming that 100% helicity corresponds to −34 000 deg cm^2 dmol^{-1} (Chen *et al.*, 1974), the overall helicity of FHA2 was calculated to be 49%. Also, we performed CD measurements on the spin-labeled mutants and found that the spectra are nearly identical to that of the wild type. We also calculated the helical content of the region corresponding to FHA2 (aa 1−127) in the native HA structure (Wilson *et al.*, 1981) as a reference and it was found to be 52%, which is close to the helical content of isolated FHA2 (49%).

Site-Specific Cys−Cys Cross-Linking. The mutational sites 63, 64, 65, and 66 occupy the **a**, **b**, **c**, and **d** positions of the trimeric coiled-coil, respectively, in the low-pH crystal structure of the proteolytically cleaved HA fragment (Bullough *et al.*, 1994). These positions are indicated in the helical wheel representing a cross section of the trimeric coiled-coil in Figure 1. Since the protein inserted into the *E. coli* membrane when it was expressed and because it was sufficiently overexpressed, the cys−cys cross-linking experiment was possible in the isolated *E. coli* membrane without further purification. For all mutants the cross-linking reaction was initiated by adding the reagent Cu(II)(phe)$_3$. The SDS−PAGE gels showing the extent of cys−cys cross-linking for individual mutants are given in Figure 4a. The incubation times were 25 s and 10 min at 37 °C. In the gels the 14 kDa molecular weight bands are from the monomeric fragment and the 28 kDa molecular weight bands correspond to the dimer formed by the cys−cys disulfide bond between two monomers. In Figure 4a it is shown that the cross-linking reaction occurred for all mutants. For F63C and I66C, we observed fast cross-linking. Assuming a coiled-coil geometry, these two residues are at internal **a** and **d** positions, respectively, for which fast cross-linking is expected. However, it is very surprising to observe extensive cross-linking for the H64C mutant which would be on the outside in a trimeric coiled-coil. Moreover, the rate of cross-linking for H64C was comparable to the rates of F63C and I66C. A coiled-coil structure would render thiol groups at least 17 Å away from one another for H64C. It is known that the cys−cys cross-linking reaction is specific and occurs only when the cysteine residues are in close proximity (within a few Å). Thus, our results suggest that the structure of this region is flexible enough for thiols at H64C from individual monomers to be able to contact each other and cross-link. On the other hand we observe only weak cys−cys cross-linking for Q65C.

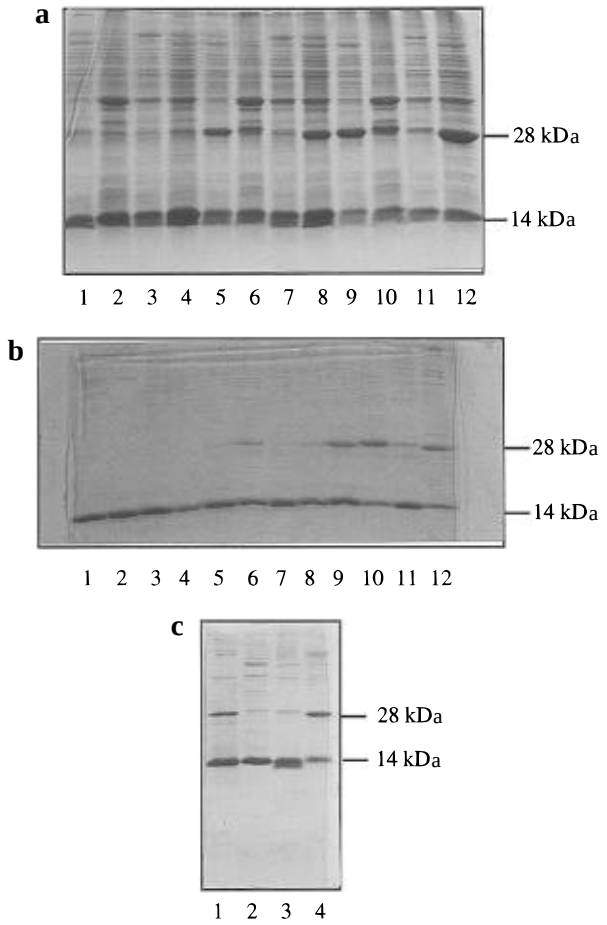

FIGURE 4: SDS−PAGE 15% gels show three different cys−cys cross-linking experiments performed on FHA2 cysteine mutants: (a) cross-linking in *E. coli* membrane before solubilization or purification (top); (b) cross-linking in 2% OG after purification (middle); and (c) natural cross-linking after 1 month of storage at −80 °C (bottom). In each case the amount of cross-linking can be seen by the intensity of the dimer (28 kDa) band. Experiments a and b were performed at 37 °C with Cu(II)(1,10-phenanthroline)$_3$ as a cross-linking catalyst. Cross-linking in c was due to exposure to ambient O_2 and the lack of a reducing agent. Lanes 1−4 in a and b are mutants at positions 63−66, respectively, before cross-linking, lanes 5−8 are positions 63−66 cross-linked for 25 s, and lanes 9−12 are positions 63−66 cross-linked for 10 min. In c lanes 1−4 are positions 63−66, respectively.

We also performed the cross-linking experiments in the OG solubilized state (Figure 4b) and in the membrane-reconstituted state as well (data not shown). We obtained similar results to those in the native *E. coli* membrane state. Again we observed extensive cross-linking for H64C, and the rate was even faster than those of F63C and I66C in OG.

We investigated the effect of the temperature on the cross-linking rates for the different cysteine mutants. At 0 °C the rate of the cross-linking for H64C in the *E. coli* membrane

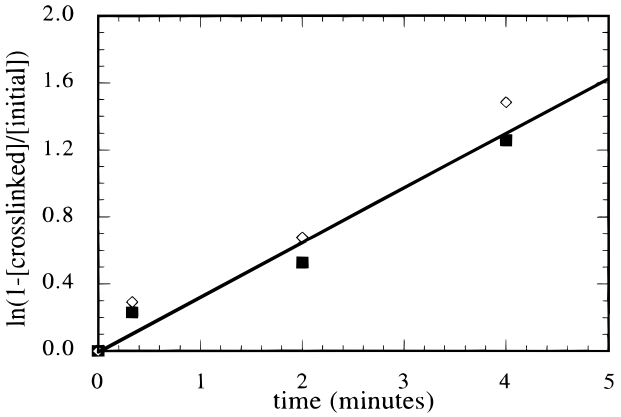

FIGURE 5: Plotting the log of cross-linked trimers as a function of time demonstrates that the cross-linking reaction is concentration independent and proceeds with a rate constant $k = 0.32\ s^{-1}$. Data points from 15 μM H64C FHA2 are marked with ■, whereas ◇ stands for 45 μM H64C. The close agreement between these two concentrations in the first 5 min indicates that the reaction is intratrimeric. At reaction times longer than 10 min the reaction approaches completion (i.e., two-thirds of the monomers have cross-linked).

was somewhat slower than that of F63C and I66C (data not shown). On the other hand, in the frozen state (−80 °C) we did not observe any appreciable cross-linking for H64C although dimers are formed for F63C and I66C (Figure 4c).

To determine whether the cross-linking reaction for H64C is intertrimeric or intratrimeric, the dependence of the initial rate on the protein concentration was examined for OG-solubilized H64C. We should expect a linear dependence of the initial rate on the protein concentration for intramolecular cross-linking. On the other hand, we would observe a quadratic dependence on the protein concentration if it is intermolecular. For H64C we found that the initial rate is linearly proportional to the concentration of the protein (Figure 5), suggesting that the reaction is intratrimeric. The progress of the cross-linking reaction fits well with a line corresponding to first-order kinetics. In Figure 5 the reaction at 15 μM protein concentration was compared with that at 45 μM protein concentration. The close agreement of the kinetics between these two concentrations again indicates that the reaction is intratrimeric.

We also determined the dimer to monomer ratio after longer reaction time. It was found that 63, 64, and 66 all approached approximately 67% dimer, which would be expected for a trimeric protein (Milligan & Koshland, 1988).

Spin-Labeling EPR. Although the cys−cys cross-linking technique is a powerful method to investigate the structure and dynamics of proteins it is limited only to the pH conditions near neutrality. Thus, this method is not applicable to the investigation of the conformation of FHA2 under low-pH conditions. Instead, spin-labeling EPR is used to probe the pH-induced conformational change since for spin-labeling EPR there is no restriction on the pH.

Three cysteine mutants, F63C, H64C, and Q65C, were labeled with MTSSL spin label. The EPR spectra were taken with the spin-labeled mutants reconstituted into phospholipid membranes. The EPR spectra under neutral and low-pH conditions are shown in Figure 6. It was noted that spin-labeled I66C aggregated during the reconstitution process for unknown reasons.

When more than two nitroxides reside nearby each other, the electron spins interact with one another through spin−

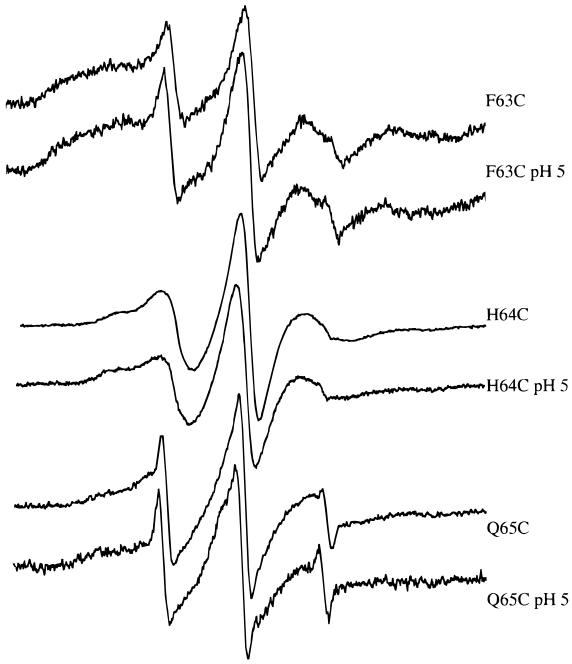

FIGURE 6: Plots of EPR spectra for the spin-labeled mutants. The scan width was 100 gauss for all spectra.

spin exchange interactions and dipolar interactions. Except in the motionally frozen state, however, the dipolar interactions usually time-average to be negligible and spin exchange is the main interaction that effectively broadens the EPR lines. For spin-labeled F63C appreciable exchange broadening was detected, indicating that the spin labels at position 63 are close to one another in the trimer. On the other hand we observe less spin exchange broadening for H64C and Q65C.

Another important parameter of the EPR spectrum for structural information is the motional broadening. If the motion of the nitroxide is restricted due to its interaction with the helical backbone or if the motion is confined due to tertiary or quaternary interactions, a broad EPR line shape with a rotational correlation time greater than 10 ns is expected. On the other hand, if the nitroxide is freely rotating without steric hindrance, a relatively sharp EPR line shape with a rotational correlation time of less than 5 ns is expected. Typically the nitroxide attached to a flexible loop or a random coil peptide exhibits such a comparatively narrow spectrum. The dependence of the EPR line shape on the environment of the nitroxide in a protein was carefully and extensively investigated by Hubbell and co-workers in the well-characterized lysozyme protein (personal communication with Dr. Hubbell). This library of EPR spectra serves as a good reference in interpreting the spectra of unknown structures.

When compared with this EPR spectral library, the EPR spectra of H64C and Q65C in the membrane at pH 7.0 (Figure 6) correspond to those of a flexible structure. The rotational correlation times are on the order of 5 ns for both spectra. Although the EPR line shapes of F63C are somewhat complicated due to exchange broadening, the rotational correlation time is estimated to be less than 10 ns (Schneider & Freed, 1989), which is faster than the typical 20 ns rotational correlation time for internal coiled-coil positions. This result again indicates that the mobility of this region is greater than expected for a well-defined coiled-coil.

Since low pH is the main cause of the conformational change to the fusion-active state of HA, it is interesting to note any pH-dependent conformational transitions in this region. In Figure 6 the EPR spectra obtained at pH 5.0 are also shown. When these spectra were compared with the neutral pH spectra, we did not observe any significant changes, suggesting that this region of the isolated HA2 domain does not undergo any conformational changes at low pH. In this experiment it was noted that low-pH EPR is only possible with reconstituted samples because the detergent-solubilized protein aggregates under acidic conditions.

DISCUSSION

In the native HA, the region containing residues 63−66 is a 28-residue long hairpin loop connecting a short α-helix in the NH_2-terminal region and a long α-helix (Wilson *et al.*, 1981). Recently it has been suggested that the stable conformation of this region is an α-helix under both neutral pH and low-pH conditions (Chen *et al.*, 1995). This supports the kinetic model for the low-pH-induced conformational change of HA (Carr & Kim, 1993) which proposes that the hairpin structure in the HA2 domain of native HA is a kinetically trapped metastable conformation. Thus, the role of the low pH is to catalyze the transition from the metastable hairpin to the stable helical coiled-coil by removing the high-energy barrier imposed by HA1−HA2 interactions. This view is also supported by the study of HA mutations that effect the onset pH of membrane fusion (Daniels *et al.*, 1985).

In this work it is shown that the region containing residues 63−66 is flexible and dynamic rather than being a well-defined coiled-coil at physiological temperatures. At 37 °C the rates of the cross-linking reaction were all comparable for 63, 64, and 66 (Figure 4a,b). This pattern was not significantly changed at 0 °C, but the rate of the cross-linking for 64 was slightly slower than at 37 °C (data not shown).

However, an increase of features consistent with a coiled-coil conformation was observed at very low temperature. In the frozen state (−80 °C) there was no natural cys−cys cross-linking (without the reagent) for 64 while there was substantial natural cross-linking for 63 and 66 (Figure 4c). This might imply that there is an equilibrium between a random coiled-coil and a well-defined coiled-coil, which could be easily shifted by thermal fluctuations.

Obtaining information about the low-pH conformation was made possible by EPR. This technique is not adversely affected by low pH, unlike cys−cys cross-linking which requires a pH near 7 for adequate oxidation of sulfur. No change in the EPR spectra of cysteine mutants upon lowering the pH to fusogenic conditions was observed. Considering that the EPR spectra are sensitive to conformational changes, this suggests that the flexible structure is the stable conformation under both neutral and low pH conditions. On the other hand, it has been previously found that synthetic peptides derived from the hairpin-loop region of the HA2 domain form a trimeric coiled-coil under low-pH conditions (Carr & Kim, 1993; Yu *et al.*, 1994). These observations may not be physiologically relevant.

The dynamic conformational state of FHA2 could be achieved through two mechanisms. First, while keeping the helical coiled-coil geometry, the helices could rotate along the helical axis with respect to one another in the trimer. In this way, thiols at each position could come close and react to form a disulfide bond. To accomplish this for position 64, however, there must be at least 100-degree rotation of the helices. This would be accomplished only by exposing a significant fraction of the hydrophobic face of the helix to the aqueous phase and by burying the hydrophilic face into the interior of the trimer. Such fluctuations may be energetically too costly to occur. The second possible mechanism could be an equilibrium between a helical conformation and a random coil conformation. Therefore, although it would be difficult for H64C to be cross-linked in a helical conformation, thiols at this position can easily come close and be cross-linked when in a flexible random coil.

CD results indicate that FHA2 is 49% helical in a detergent solution. It is likely that the apolar NH_2-terminal fusion peptide region is bound to the detergent micelle and takes an α-helical conformation as do many hydrophobic peptides in detergent. In fact it was shown that a synthetic peptide derived from this region is α-helical in a membrane environment (Ishiguro *et al.*, 1993). Taken together, it appears that a significant portion of FHA2 is not in an α-helical conformation, somewhat consistent with the finding that the region containing residues 63−66 is flexible and may not be in a well-defined helical conformation. In contrast, a fragment of HA2 without the fusion peptide region (aa 38−175) was found to be more than 80% helical by CD measurement (Chen *et al.*, 1995). For FHA2 the insertion of the fusion peptide region to a highly dynamic bilayer or micelle may contribute to the dynamic fluctuations of the structure of FHA2.

Recently a fusion intermediate for HA-induced membrane fusion was proposed by Wiley and co-workers (Wharton *et al.*, 1995). This model is based on X-ray crystallographic studies of proteloytically cleaved HA2 fragments (Bullough *et al.*, 1994) and electron microscopic studies of various HA2 fragments and antibody-bound HA fragments (Wharton *et al.*, 1995). In this model the long HA2 coiled-coil rod is bound to the target membrane with an orientation perpendicular to the membrane surface. Consequently, this model is left with a more than a 100 Å gap separating the viral and endosomal membranes. However, fusion seems to require the apposition of the two membranes (Yu *et al.*, 1994). How could this apposition be accomplished? Supposing that the proposed fusion intermediate does exist in the fusion process, then the expected flexible region would be in the middle of the coiled-coil rod. This flexibility would provide a mechanism for apposition: the region may bend or splay apart to bring the two membranes together. HA2 is known to have a certain amount of flexibility in the COOH-terminal stem region. However, flexibility in the COOH-terminal stem region of HA2 alone could be insufficient to allow rearrangement of the bridging spikes, which may be required for apposition (Wharton *et al.*, 1995).

Apposition and fusion of two membranes are energetically costly events. The membranes have to overcome the high energy-of-hydration barrier (Leikin *et al.*, 1993) and the bilayer-bending energy barrier (Siegel, 1993). What allows the membranes to overcome these fusion barriers? Lear and DeGrado (1987) have shown that a 20-residue synthetic peptide derived from the HA2 fusion peptide bound to one phospholipid vesicle will trigger fusion with a second vesicle. In this process it is likely that the simultaneous interaction of the peptide with two membranes is sufficient to overcome the barriers to fusion. Likewise, for HA the simultaneous interaction of the fusion peptide region with two membranes

might be sufficient to accomplish fusion. Substantial flexibility of the protein structure may be required to facilitate this cross-bridging of the two membranes by the fusion peptide. This apposition may be followed by the formation of a hemifusion intermediate (Kemble *et al.*, 1994) and a fusion pore (White, 1992).

Another interesting observation is that although FHA2 binds to the membrane at pH 7, it does not trigger fusion until the pH is lowered to ~5 (unpublished data). Such an observation is consistent with previous studies showing that there may be additional steps requiring low pH between a protein conformational change accompanied by the dissociation of the HA1 domain and the merging of the two membranes (Nebel *et al.*, 1995; Krumbiegel *et al.*, 1994).

The fact that the rate of cys−cys cross-linking for H64C is comparable to that of F63C suggests that the frequency of approach of thiols from individual monomers is comparable for these two sites. In contrast, it is interesting to observe that the spectral broadening due to spin−spin interactions in the EPR spectrum of spin-labeled H64C is much less than that of spin-labeled F63C. Spin−spin interactions are functions of the average distance between nitroxides. Thus this EPR result may suggest that the average spatial separations, in time, between nitroxides attached to position 64 are farther than those between nitroxides attached to position 63. It is also interesting to observe a much slower cross-linking rate for Q65C than that of H64C. This may simply be due to steric hindrances which prevent thiols on Q65C from approaching within a few Å.

In summary, it has been shown, using the methods of site-specific cross-linking and spin-labeling EPR, that the stable conformation of the region containing residues 63−66 is flexible and dynamic, implying that there may be an equilibrium between an extended random coil and an α-helical conformation at physiological temperatures. The flexibility and dynamic structure of this region may have important implications for the mechanism of HA-induced membrane fusion. For example, flexibility may be required for the apposition of the viral and cell membranes. Also, we have shown that cross-linking and EPR, if combined in a proper way, can yield more interesting implications for membrane proteins than when they are used separately.

ACKNOWLEDGMENT

We would like to thank Dr. Peter S. Kim for sending us the plasmid expressing the soluble portion of HA2 (aa 33−127).

REFERENCES

Bullough, P. A., Hughson, F. M., Skehel, J. J., & Wiley, D. C. (1994) *Nature (London) 371*, 37−43.
Carr, C. M., & Kim, P. S. (1993) *Cell 73*, 823−832.
Chen, J., Wharton, S. A., Weissenhorn, W., Calder, L. J., Hughson, F. M., Skehel, J. J., & Wiley D. C. (1995) *Proc. Natl. Acad. Sci. U.S.A. 79*, 968−972.
Chen, Y.-H., Yang, J. T., & Chau, K. T. (1974) *Biochemistry 13*, 3350−3359.
Daniels, R. S., Downie, J. C., Hay, A. J., Knossow, M., Skehel J. J., Wang, M. L., & Wiley D. C. (1985) *Cell 40*, 431−439.
Doms, R. W., & Helenius, A. (1986) *J. Virol. 60*, 833−39.
Falke, J. J., & Koshland, D. E., Jr. (1987) *Science 237*, 1596−1600.
Gething, M. J., Doms, R. W., York, D., & White, J. (1986) *J. Cell Bol. 102*, 11−23.
Habeeb, A. F. S. A., & Hiramoto, R. (1968) *Arch. Biochem. Biophys. 126*, 16−26
Hubbell, W. L., & Altenbach, C. (1994) Site-directed spin labeling of membrane proteins, in *Membrane Protein Structure: Experimental Approaches* (White, S., Ed.) Oxford University Press, New York.
Ishiguro, R., Kimura N., & Takahashi, S. (1993) *Biochemistry 32*, 9792−9797.
Kemble, G. W., Danieli, T., & White, J. M. (1994) *Cell 76*, 383−391.
Krumbiegel, M., Hermann, A., & Blumenthal, R. (1994) *Biophys. J. 67*, 2355−2360.
Kunkel, T. A. (1985) *Proc. Natl. Acad. Sci. U.S.A. 82*, 488−492.
Lear, J. D., & DeGrado, W. F. (1987) *J. Biol. Chem. 262*, 6500−6505.
Leikin, S., Parsegian, V. A., Rau, D. C., & Rand, R. P. (1993) *Annu. Rev. Phys. Chem. 44*, 369−395.
Maltin, K. S., Reggio, H., Helenius, A., & Simons, K. (1981) *J. Cell. Biol. 91*, 601−613.
Millhauser, G. L. (1992) *Trends Biochem. Sci. 17 (11)*, 448−452.
Milligan, D. L., & Koshland, D. E., Jr. (1988) *J. Biol. Chem. 263*, 6268−6275.
Nebel, S., Bartoldus, I., & Stegmann, T. (1995) *Biochemistry 34*, 5705−5711.
Puri, A., Booy, F. P., Doms, R. W., White, J. M., & Blumenthal, R. (1990) *J. Virol. 64*, 3824−3832.
Rabenstein, M., & Shin, Y. K. (1995a) *Biochemistry 34*, 13390−13397.
Rabenstein, M., & Shin, Y. K. (1995b) *Proc. Natl. Acad. Sci. U.S.A. 92*, 8239−8243.
Ruigrok, R. W. H., Wrigley, N. G., Calder, L. J., Cusack S., Wharton, S. A., Brown, E. B., & Skehel, J. J. (1986) *EMBO J. 5*, 41−49.
Schneider, D. J., & Freed, J. H. (1989) in *Biological Magnetic Resonance* (Berliner, L. J., & Ruben, J., Eds.) Vol. 8, pp 1−76, Plenum, New York.
Siegel, D. P. (1993) *Biophys. J. 65*, 2124−2140.
Skehel, J. J., Bayley, P. M., Brown, E. B., Martin, S. R., Waterfield, M. D., White, J. M., Wilson, I. A., & Wiley, D. C., (1982) *Proc. Natl. Acad. Sci. U.S.A. 79*, 968−972.
Stegmann, T., & Helenius, A. (1993) in *Viral Fusion Mechanisms* (Bentz, J., Ed.), pp 89−111, CRC Press, Inc., Boca Raton, FL.
Stegmann, T., White, J. M., & Helenius, A. (1990) *EMBO J 9*, 4231−4241.
Stegmann, T., Delfino, J. M., Richards, F. M., & Helenius, A. (1991) *J. Biol. Chem. 266*, 18404−18410.
Tsurudome, M., Glueck, R., Graf, R., Falchetto, R., Schaller, U., & Brunner, J. (1992) *J. Biol. Chem. 267*, 20225−20232.
Wharton, S. A., Calder, L. J., Ruigrok, R. W. H., Skehel, J. J., Steinhauer, D. A., & Wiley, D. C. (1995) *EMBO J. 14*, 240−246.
White, J. M. (1992) *Science 258*, 917−924.
White, J. M., & Wilson, J. A. (1987) *J. Cell Biol. 105*, 2887−2896.
Wiley, D. C., & Skehel, J. J. (1987) *Annu. Rev. Biochem. 56*, 365−394.
Wilson I. A., & Wiley D. C. (1982) *Proc. Natl. Acad. Sci. U.S.A. 79*, 968−72.
Wilson, I. A., Skehel, J. J., & Wiley, D. C. (1981) *Nature (London) 289*, 366−373.
Yu, H., Kono, M., Mckee, T. D., & Oprian, D. D. (1995) *Biochemistry 34*, 14963−14969.
Yu, Y. G., King, D. S., & Shin, Y. K. (1994) *Science 266*, 274−276.

BI960332+